Zhou *et al. Biology Direct* (2024) 19:117
https://doi.org/10.1186/s13062-024-00568-w

Biology Direct

RESEARCH Open Access

miPEP31 alleviates sepsis development by regulating Chi3l1-dependent macrophage polarization

Yu Zhou[1†], Yuan Yuan[1†], Xuanqi Yao[1†], Lin Wang[1], Liangfang Yao[1], Daolin Tang[2], Feng Chen[1*] and Jinbao Li[1*]

Abstract

Background Sepsis is a severe condition characterized by multiple organ dysfunction resulting from an imbalanced host immune response to infections. miRNAs play a crucial role in regulating various biological processes. However, the precise role of miR-31 in the immunopathology of sepsis remains poorly understood.

Methods The concentration of hsa-miR-31-5p in patients with sepsis (both survivors and non-survivors) and healthy individuals was assayed. Using an experimental sepsis model of caecal ligation and puncture (CLP), the impact of mmu-miR-31-5p on survival, organ injury, and inflammation was evaluated. Additionally, the effect of mmu-miR-31-5p on macrophage polarization through Chi3l1 was investigated. Lastly, the therapeutic effects of miPEP31 on experimental sepsis were examined.

Results The results of miRNA sequencing (miRNA-seq) and quantitative polymerase chain reaction (q-PCR) analyses identified hsa-miR-31-5p as a potential biomarker for patients with sepsis, with non-survivors showing higher levels of hsa-miR-31-5p in peripheral blood mononuclear cells (PBMCs) compared to survivors. Functional studies conducted on peritoneal elucidated macrophages (PEMs) demonstrated that mmu-miR-31-5p inhibits M2 polarization in macrophages by downregulating Chi3l1. The utilization of miPEP31 as a therapeutic intervention had a substantial impact on reducing mortality rates, mitigating organ damage, inducing macrophage polarization towards the M2 phenotype, and suppressing the inflammatory response in murine models of severe sepsis.

Conclusions The suppression of miR-31 in sepsis plays a protective role in the host defense response by upregulating Chi3l1, highlighting the potential therapeutic efficacy of miPEP31 in sepsis treatment.

†Yu Zhou, Yuan Yuan and Xuanqi Yao contributed equally to this work.

*Correspondence:
Feng Chen
smmuchenfeng@163.com
Jinbao Li
lijinbaoshanghai@163.com

Full list of author information is available at the end of the article

Graphical abstract

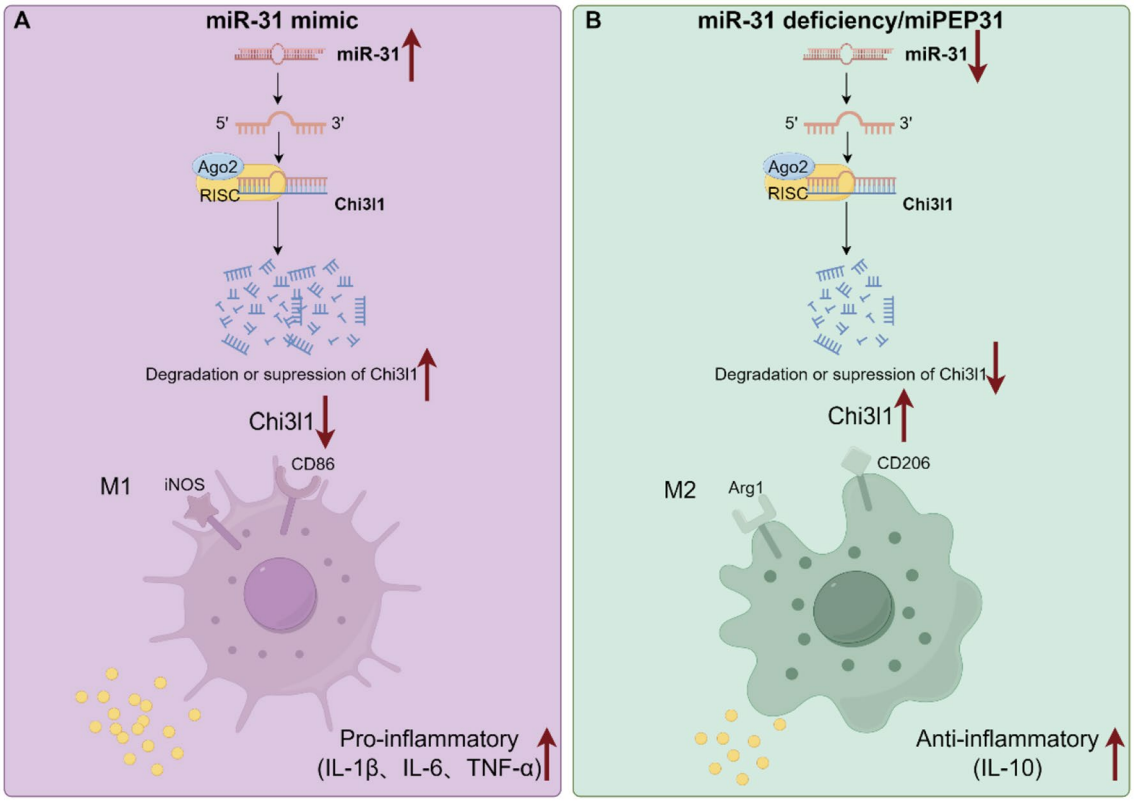

Keywords Sepsis, Macrophage polarization, miPEP31, Chi3l1

Introduction

Sepsis, a critical medical condition, arises from the concurrent presence of infection and a widespread inflammatory response, resulting in profound disruptions to both the immune system and organ function [1]. Despite considerable efforts to implement early preventive and bundled interventions, morbidity and mortality rates remain high, with sepsis persisting as the primary cause of death among critically ill patients in clinical settings [2, 3]. The underlying mechanism propelling the onset and progression of sepsis predominantly involves immune dysregulation [4]. During the initial phase of sepsis, the host's immune response is characterized by a surge in inflammatory mediators, which damage both tissues and immune cells. This inflammatory cascade leads to a subsequent stage of sepsis marked by host immunosuppression. Therefore, the primary objective of immunotherapy for septic patients is to restore and maintain the delicate balance of the host's immune system.

Macrophages exhibit remarkable plasticity, enabling them to transition between distinct functional states known as M1 and M2 phenotypes. M1 macrophages, or classically activated macrophages, typically arise in response to pro-inflammatory stimuli, such as interferon-gamma (IFN-γ) and lipopolysaccharide (LPS) [5]. These cells excel at producing inflammatory cytokines and reactive oxygen species, playing a pivotal role in the initial defense against pathogens. Conversely, M2 macrophages, termed alternatively activated macrophages, emerge in response to anti-inflammatory cues, such as interleukin-4 (IL-4) and interleukin-13 (IL-13). These cells contribute to tissue repair, inflammation resolution, and immune regulation. In sepsis, macrophage polarization becomes dysregulated, leading to an imbalance between the pro-inflammatory M1 and anti-inflammatory M2 phenotypes. This dysregulation contributes to ongoing inflammation, tissue injury, and organ dysfunction observed in severe sepsis and septic shock. Understanding and modulating macrophage polarization hold promise as therapeutic avenues for attenuating the detrimental effects of sepsis and enhancing patient outcomes [5].

MicroRNAs (miRNAs) are small, endogenous, noncoding RNAs that function to post-transcriptionally inhibit gene expression by binding to the 3'untranslated region (3'UTR) of target genes [6]. Accumulating evidence demonstrates the pivotal role of miRNAs in regulating diverse

pathophysiological processes, including cell proliferation, metabolism, apoptosis, and organ development. Importantly, dysregulation of miRNAs has been implicated in clinical manifestations and inflammation, highlighting their potential as therapeutic targets for sepsis [7–9]. Indeed, miRNAs modulate macrophage polarization and its subsequent impact on inflammation [10]. However, the precise role of miRNA-mediated macrophage polarization in sepsis remains incompletely understood.

In this study, we screened miRNAs in septic and healthy individuals, identifying hsa-miR-31-5p (mmu-miR-31-5p in mice) as a previously unrecognized biomarker for sepsis severity prediction. Utilizing miR-31 knockout mice and biochemical assays in primary macrophages, we demonstrated that miR-31 depletion protects against sepsis by targeting the cytokine chitinase-3-like 1 (Chi3l1, YKL-40/CHI3L1 in humans), promoting M2 macrophage polarization. These findings may provide a novel strategy for the treatment of sepsis.

Results

Hsa-miR-31-5p correlates with inflammation and worsened prognosis in sepsis patients

This study utilized miRNA-seq to identify potential biomarkers for sepsis in a pilot cohort, and employed qPCRs to validate the association of miRNAs with sepsis in a separate cohort. Furthermore, a murine model of caecal ligation and puncture (CLP)-induced sepsis was utilized to assess the therapeutic impact of miPEP31 (Fig. 1A). To delve deeper, peripheral blood samples were initially procured from three sepsis patients who admitted to the intensive care unit (ICU) without any intervention and three healthy controls. Relative to healthy controls, septic patients exhibited significant downregulation of five microRNAs (hsa-miR-4464, hsa-miR-31-5p, hsa-miR-508-3p, hsa-miR-31-3p and hsa-miR-150-5p) and upregulation of three microRNAs (hsa-miR-183-3p, hsa-miR-2115-3p and hsa-miR-96-5p) (Fig. 1B and C), utilizing $P<0.05$ as a cutoff threshold. Subsequently, additional blood samples were collected from ten sepsis patients to assess disease severity.

The sequential organ failure assessment (SOFA) score is a tool used to assess the severity of organ dysfunction in critically ill patients, particularly those with sepsis or other forms of systemic inflammatory response syndrome. We unveiled a substantial positive correlation between the SOFA score and hsa-miR-31-5p levels in peripheral blood (Fig. 1D). In sepsis patients, interleukin-6 (IL-6) plays a crucial role as a key mediator of the inflammatory response. Furthermore, hsa-miR-31-5p levels exhibited a positive association with IL-6 (Fig. 1E), while no statistically significant correlation was observed between other microRNAs and SOFA or IL-6 levels (Fig. S1). Additionally, hsa-miR-31-5p expression was elevated in deceased patients compared to survivors (Fig. 1F), suggesting a potential association with disease severity in sepsis cases. The expression level of mmu-miR-31-5p was found to be decreased in septic mice and increased in mice with high-grade sepsis compared to those with mid-grade sepsis (Fig. 1G).

Overall, these clinical studies suggest that elevated expression of hsa-miR-31-5p may indicate an intensified inflammatory response and an unfavorable prognosis in patients with sepsis.

Deletion of miR-31 protects against experimental sepsis in mice

The CLP model serves as a widely employed experimental model for investigating sepsis. To elucidate the specific role of mmu-miR-31-5p in sepsis, a CLP-induced sepsis model was established using miR-31 knockout mice. We confirmed a significant reduction in mmu-miR-31-5p levels in the peripheral blood mononuclear cells (PBMCs) and lungs of miR-31 knockout mice (Fig. S2). Comparative analysis revealed that miR-31 knockout mice exhibited significantly elevated survival rates and diminished murine sepsis scores in contrast to wild-type controls (Fig. 2A and B). Moreover, histopathological assessment demonstrated a lower lung injury score in miR-31$^{-/-}$ mice compared to wild-type (WT) mice (Fig. 2C and D), implying a potentially improved prognosis in septic mice lacking miR-31. After 12 h post-CLP, the extent of liver and kidney injury appeared to be less pronounced compared to lung injury (Fig. S3).

Arginase-1 (Arg1) plays a crucial role in inflammation modulation by fostering an anti-inflammatory milieu through M2 macrophage polarization and the regulation of arginine metabolism. Immunofluorescence and q-PCR analysis revealed an upregulation of *Arg1* expression in the lungs of miR-31$^{-/-}$ septic mice (Fig. 2E and F). Furthermore, the expression levels of inflammatory cytokines (IL-10, IL-1β, IL-6, and TNF-α) were assessed in PBMCs of CLP-induced septic mice, the levels of pro-inflammatory factors were reduced and anti-inflammatory factors were elevated in septic mice lacking miR-31 (Fig. 2G).

The findings indicate that macrophages lacking miR-31 in mice exhibited a tendency toward differentiation into an M2 phenotype, thereby resulting in a diminished inflammatory response.

miR-31 inhibits macrophage differentiation into M2 phenotype

Next, we investigated the impact of miR-31 on macrophage polarization in response to LPS, a classical pathogen-associated molecular pattern (PAMP) produced by gram-negative bacteria. Our study revealed that the most pronounced reduction in mmu-miR-31-5p levels

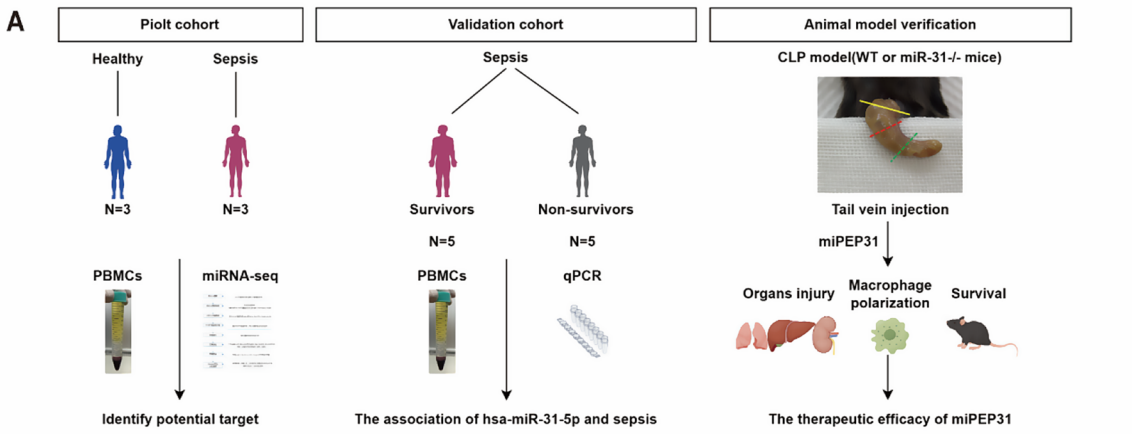

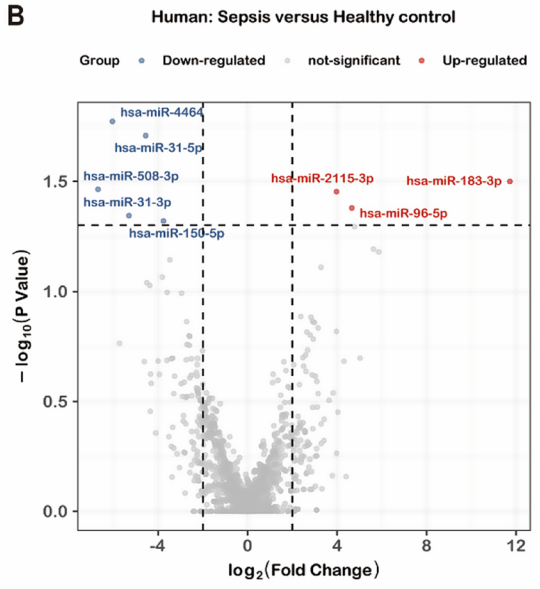

C

MicroRNAs with significant fold change (sepsis versus healthy control)

Systematic name	P values	Fold change
A. Selection of down-regulated genes		
hsa-miR-4464	0.016858614	0.015133919
hsa-miR-31-5p	0.019564295	0.042403526
hsa-miR-508-3p	0.034332478	0.009683064
hsa-miR-31-3p	0.04522981	0.025309963
hsa-miR-150-5p	0.047872093	0.073635488
B. Selection of up-regulated genes		
hsa-miR-183-3p	0.031608528	Inf
hsa-miR-2115-3p	0.035184676	15.68716924
hsa-miR-96-5p	0.04172338	25.20587003

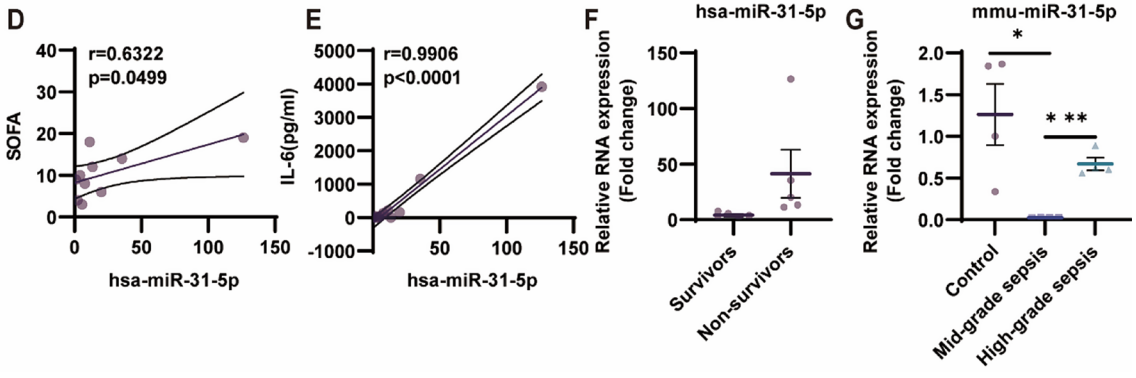

Fig. 1 Hsa-miR-31-5p correlates with inflammation and worsened prognosis in sepsis patients. **A**. miRNA-seq was employed to identify potential biomarkers for sepsis in a pilot cohort, and qPCRs were used to confirm the association of miRNAs and sepsis in a validation cohort. A murine model of CLP-induced sepsis was employed to evaluate the therapeutic impact of miPEP31. **B** and **C**. In comparison to non-septic individuals ($n=3$), five microRNAs significantly downregulated and three microRNAs significantly upregulated in these septic patients ($n=3$). **D**. The SOFA score and hsa-miR-31-5p levels in peripheral blood of septic patients was positively related ($n=10$, $P<0.05$). **E**. The IL-6 was also positively related with hsa-miR-31-5p levels in peripheral blood of septic patients ($n=10$, $P<0.0001$). **F**. The expression level of hsa-miR-31-5p was higher in death patients ($n=5$) compared to survivors ($n=5$). **G**. The expression level of mmu-miR-31-5p was lower in septic mouse, while it was higher in the mouse of high-grade sepsis compared to mid-grade sepsis ($n=3$).The data are presented as the mean ± SEM, $^{*}P<0.05$, $^{***}P<0.001$

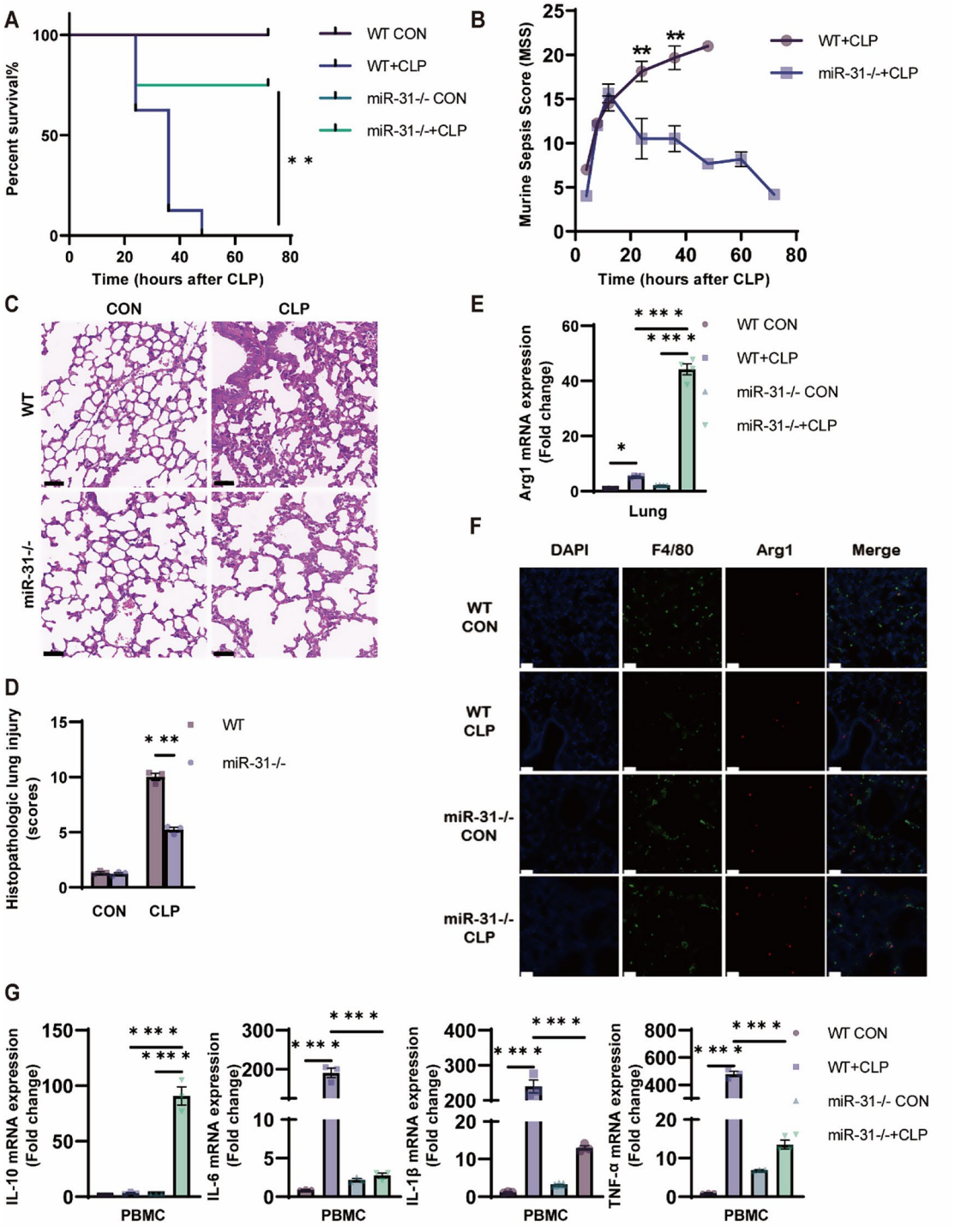

Fig. 2 Deletion of miR-31 protects against experimental sepsis in mice. **A**. The deletion of miR-31 in mice increased the survival rate of mice with CLP (21-gauge needle)-induced sepsis (the data are presented as the mean ± SEM, $n = 8$, mice per group; $^{**}P < 0.01$, Kaplan–Meier survival analysis). **B**. Effects of miR-31 deletion on murine sepsis score (MSS) in mice with sepsis. Sepsis was induced by CLP (21-gauge needle) (the data are presented as the mean ± SEM, $n = 8$, mice per group; $^{**}P < 0.01$). **C** and **D**. Lung tissues of mice with CLP-induced sepsis were stained with hematoxylin and eosin (12 h; scale bars, 50 μm), and the histopathologic lung injury score in miR-31$^{-/-}$ and WT mice were assessed. **E**. The mRNA expression of Arg1 in lung tissues of WT and miR-31$^{-/-}$ mice with CLP-induced sepsis were assayed. **F**. Immunofluorescence staining of lung sections for the macrophage marker F4/80 (green), Arg1(red) and DAPI (blue) (12 h; scale bar, 50 μm). **G**. The mRNA expression of IL-10, IL-1β, IL-6 and TNF-α in PBMCs of mice with CLP were detected.The data are presented as the mean ± SEM, $n = 3$, $^{*}P < 0.05$, $^{**}P < 0.01$, $^{***}P < 0.001$, $^{****}P < 0.0001$

occurred after 48 h of LPS stimulation at a concentration of 100 ng/ml (Fig. S4). Macrophages lacking miR-31 exhibited a greater propensity to differentiate into M2 macrophages following exposure to LPS stimulation (100 ng/ml) for 48 h compared to wild-type macrophages (Fig. 3A). Additionally, the ablation of miR-31 resulted in increased phagocytic capabilities of macrophages in an in vitro environment (Fig. 3B). Moreover, the expression levels of M1 markers in peritoneal elucidated macrophages (PEMs) obtained from miR-31$^{-/-}$ mice after exposure to 100 ng/ml LPS for 48 h exhibited a reduction, whereas M2 markers showed an increase in comparison to wild-type mice (Fig. 3C, D and E). Moreover, the concentrations of pro-inflammatory cytokines (IL-1β, IL-6, and TNF-α) in PEMs derived from miR-31$^{-/-}$ mice were found to be reduced after being exposed to 100 ng/ml LPS for 48 h, in contrast to wild-type mice. In contrast, the levels of the anti-inflammatory cytokine IL-10 were observed to increase in the PEMs isolated from miR-31$^{-/-}$ mice (Fig. 3F). Furthermore, our study demonstrated the regulatory impact of miR-31-5p on PEMs. Upon transfection with miR-31-5p mimics, our results indicated a significant upregulation of miR-31-5p (Fig. S5) and there was an increase in M1 markers and a decrease in M2 markers in miR-31-5p-overexpressing PEMs upon LPS stimulation (Fig. 3G, H and I). Furthermore, the levels of pro-inflammatory cytokines (IL-1β, IL-6, and TNF-α) were elevated in miR-31-5p-overexpressing PEMs following a 48-hour exposure to 100 ng/ml LPS. In contrast, a decrease in the levels of the anti-inflammatory cytokine IL-10 was noted in miR-31-5p-overexpressing PEMs (Fig. 3J).

These findings suggest that miR-31 hinders the M2 polarization of macrophages, thereby promoting an enhanced inflammatory response.

Chi3l1, downstream of miR-31, promotes M2 macrophage polarization

The mRNA target can undergo cleavage by miRNA through full complementarity with the target gene or translation inhibition through partial complementarity. Additionally, a single miRNA can target multiple genes. To elucidate the specific targets recognized by miR-31 during macrophage polarization, we conducted RNA-seq analysis on PEMs isolated from wild-type and miR-31$^{-/-}$ mice following stimulation with 100 ng/ml LPS for 48 h. This analysis revealed 169 upregulated genes and 138 downregulated genes in miR-31$^{-/-}$ mice compared to wild-type mice. Among these genes, Chi3l1 exhibited the upregulation in miR-31$^{-/-}$ PEMs following LPS treatment (Fig. 4A).

Chi3l1, also known as BRP-39 in mice and YKL-40/CHI3L1 in humans, is a secretory glycoprotein categorized within a heterogeneous group of glycosidases [11]. It acts as a signaling mediator in various bodily fluids and tissues, orchestrating a wide range of immune and inflammatory responses through interactions with specific cell surface receptors and subsequent signaling pathways [12]. Within macrophages, Chi3l1 may undergo upregulation during the terminal stages of cellular maturation to facilitate the transition into M2 macrophages [13–15]. Therefore, we posited that the marked elevation of Chi3l1 could potentially be modulated by miR-31 to influence macrophage polarization. Subsequently, a Chi3l1 overexpression plasmid was constructed to augment Chi3l1 expression (Fig. 4B), and siRNA was employed to suppress Chi3l1 expression (Fig. 4C). Chi3l1 levels increased most significantly at 48 h of stimulation with 100 ng/ml of LPS (Fig. S6). Subsequent experiments indicated that Chi3l1 overexpression induces M2 differentiation in PEMs isolated from wild-type mice stimulated with 100 ng/ml LPS for 48 h (Fig. 4D), whereas Chi3l1 knockdown inhibits M2 differentiation (Fig. 4E).

These results emphasize the significant role of Chi3l1, a downstream target of miR-31, in the regulation of macrophage polarization.

miR-31 regulates macrophage polarization to M2 through Chi3l1

Next, we examined the impact of Chi3l1 and miR-31 on macrophage polarization. We demonstrated a significant increase in the mRNA expression of Chi3l1 in PBMCs from miR-31$^{-/-}$ mice subjected to CLP compared to wild-type mice (Fig. 5A). Additionally, in vitro experiments showed a significant elevation in the mRNA and protein levels of Chi3l1 in PEMs isolated from miR-31$^{-/-}$ mice following stimulation with 100 ng/ml LPS for 48 h, contrasting with wild-type mice (Fig. 5B, C and D). Moreover, the inhibition of Chi3l1 reversed M2 polarization induced by miR-31 knockout (Fig. 5E). Additionally, the mRNA and protein expression of Chi3l1 in miR-31-5p-overexpressing PEMs stimulated with LPS exhibited a notable decrease (Fig. 5F, G, H). The overexpression of Chi3l1 reversed the M1 polarization induced by miR-31-5p mimic (Fig. 5I).

These findings indicated that miR-31 plays a role in the regulation of macrophage polarization towards the M2 phenotype via Chi3l1.

miR-31-5p directly inhibits CHI3L1

To further investigate the specific mechanism underlying the regulation of CHI3L1 by miR-31-5p, we conducted pertinent experiments utilizing 293T cells. miR-31-5p modulates transcription through promoter binding. The website query predicted the complementary sequences between hsa-miR-31-5p and CHI3L1 3′ UTR (Fig. 6A). We developed a luciferase reporter incorporating a portion of the human CHI3L1 promoter to assess the

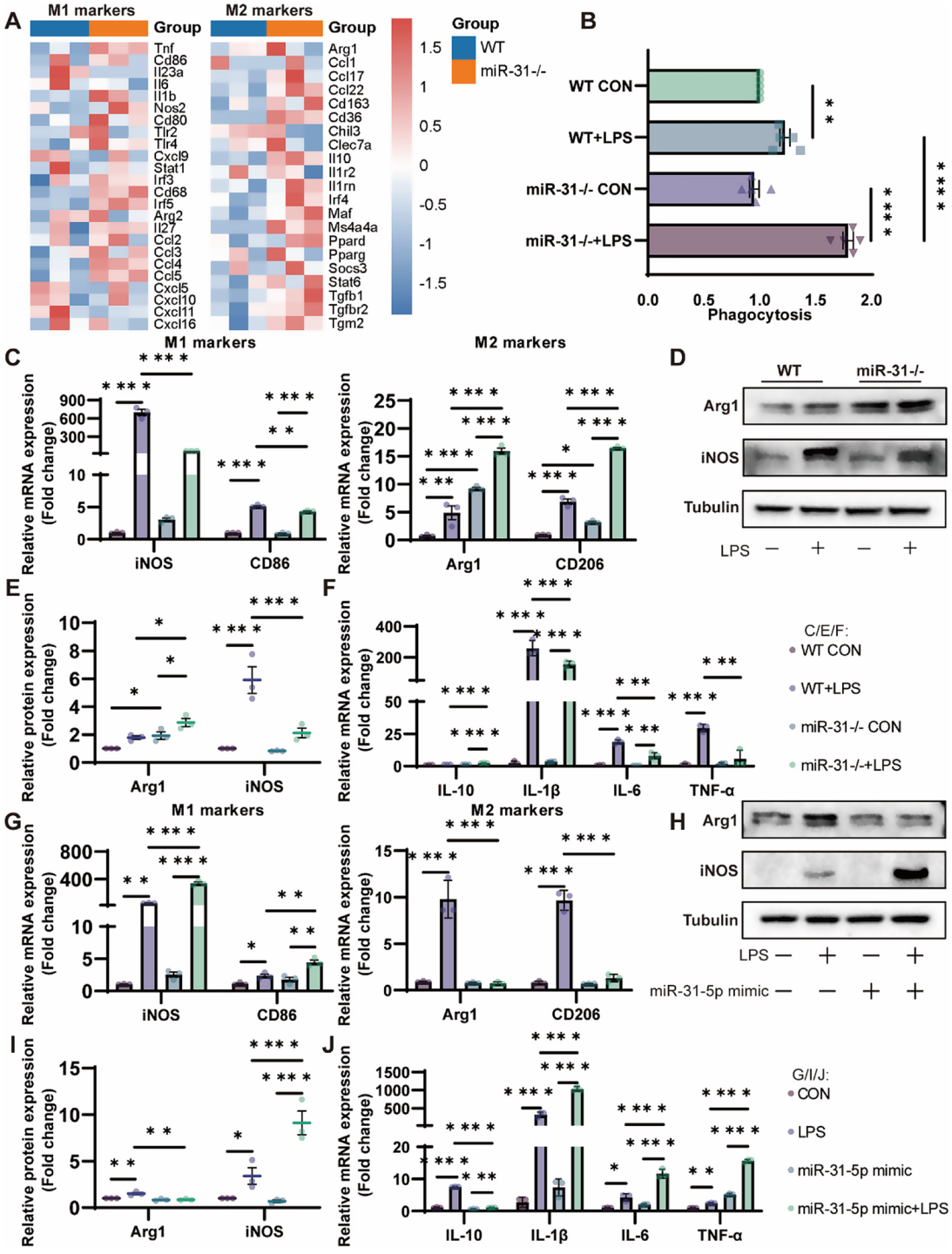

Fig. 3 miR-31 inhibits macrophage differentiation into M2 phenotype. **A**. Heatmap of macrophages makers changes in PEMs isolated from WT and miR-31$^{-/-}$ mice under LPS stimulation (100 ng/ml) for 48 h. **B**. miR-31 knockout facilitated the phagocytosis of macrophages in vitro ($n=5$). **C**. The mRNA expression of iNOS, CD86, Arg-1 and CD206 from PEMs isolated from WT and miR-31$^{-/-}$ mice stimulated with or without 100 ng/ml LPS for 48 h were assayed. **D** and **E**. The protein expression of Arg-1 and iNOS from PEMs isolated from WT and miR-31$^{-/-}$ mice stimulated with or without 100 ng/ml LPS for 48 h were detected. **F**. The mRNA expression of IL-10, IL-1β, IL-6 and TNF-α from PEMs isolated from WT and miR-31$^{-/-}$ mice stimulated with or without 100 ng/ml LPS for 48 h were assayed. **G**. The mRNA expression of Arg-1, CD206, iNOS and CD86 from PEMs in the control group and miR-31-5p overexpression group after LPS (100 ng/ml) stimulation for 48 h were detected. **H** and **I**. The protein expression of Arg-1 and iNOS from PEMs in the control group and miR-31-5p overexpression group after LPS (100 ng/ml) stimulation for 48 h were assayed. **J**. The mRNA expression of IL-10, IL-1β, IL-6 and TNF-α from PEMs in the control group and miR-31-5p overexpression group after LPS (100 ng/ml) stimulation for 48 h were detected. The data are presented as the mean ± SEM. $n=3$, $^{*}P<0.05$, $^{**}P<0.01$, $^{***}P<0.001$, $^{****}P<0.0001$

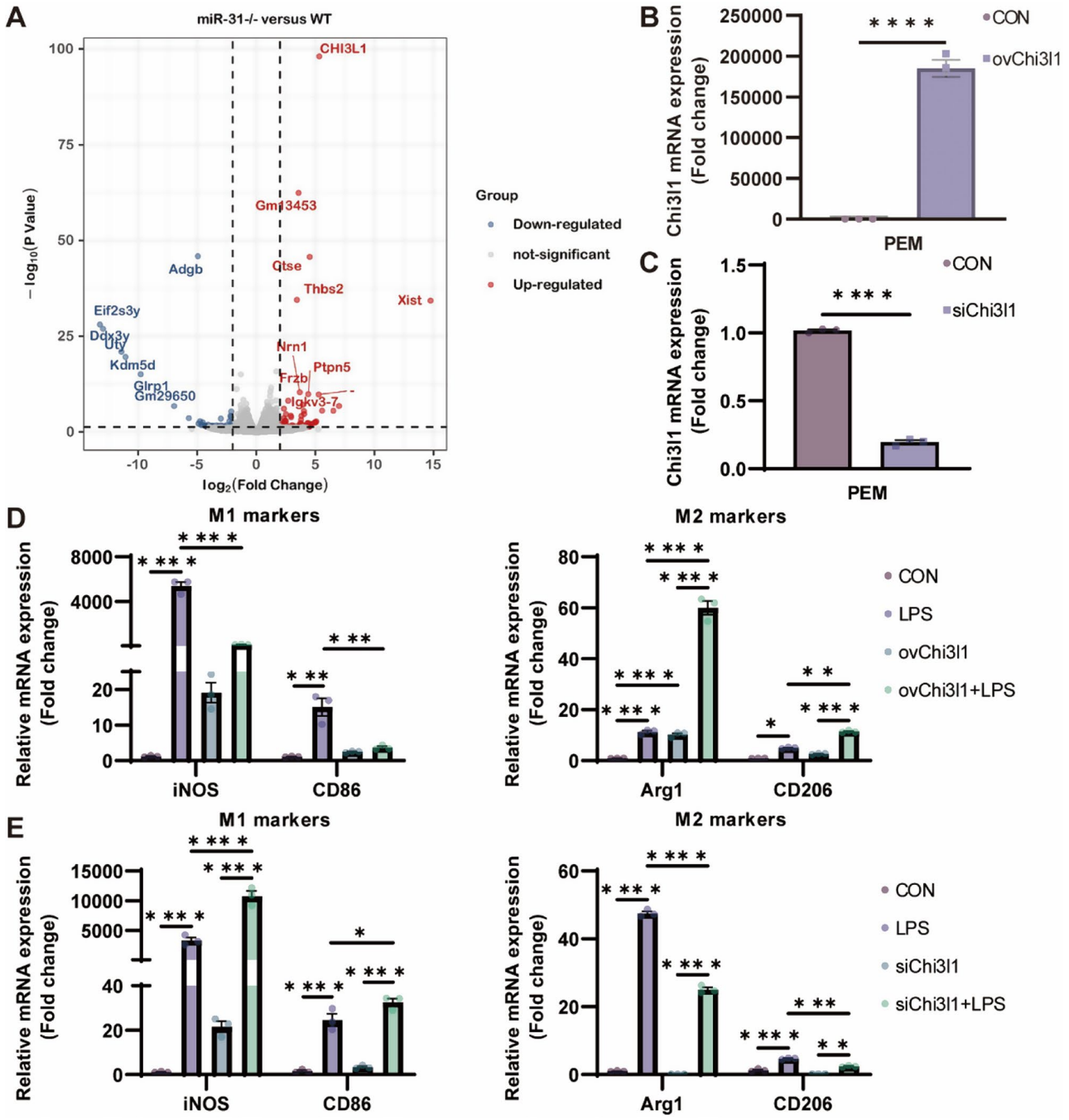

Fig. 4 Chi3l1, downstream of miR-31, promotes M2 macrophage polarization. **A**. The result of RNA-seq in PEMs isolated from WT and miR-31$^{-/-}$ mice stimulated with 100 ng/ml LPS for 48 h. **B**. The mRNA expression of Chi3l1 in Chi3l1-overexpressing PEMs was assayed. **C**. The mRNA expression of Chi3l1 in Chi3l1-underexpressing PEMs was measured. **D**. The Chi3l1 overexpression plasmid to increase the expression of Chi3l1 in PEMs isolated from WT mice, then the mRNA expression of iNOS, CD86, Arg1 and CD206 in PEMs with or without 100 ng/ml LPS for 48 h were detected. **E**. The siRNA was used to inhibit the expression of Chi3l1, the mRNA expression of iNOS, CD86, Arg1 and CD206 in Chi3l1-underexpresssing PEMs stimulated with or without 100 ng/ml LPS for 48 h were assayed. The data are presented as the mean ± SEM. $n = 3$, $^{*}P < 0.05$, $^{**}P < 0.01$, $^{***}P < 0.001$, $^{****}P < 0.0001$

influence of hsa-miR-31-5p on promoter activity in 293T cells. The findings demonstrated that the introduction of a hsa-miR-31-5p mimic resulted in a dose-dependent decrease in CHI3L1 promoter activity (Fig. 6B), suggesting that hsa-miR-31-5p regulates transcription by interacting with the CHI3L1 promoter.

The RNA-induced silencing complex (RISC) serves as a crucial mediator for miRNAs in modulating target genes. The AGO protein, a central component of RISC, plays

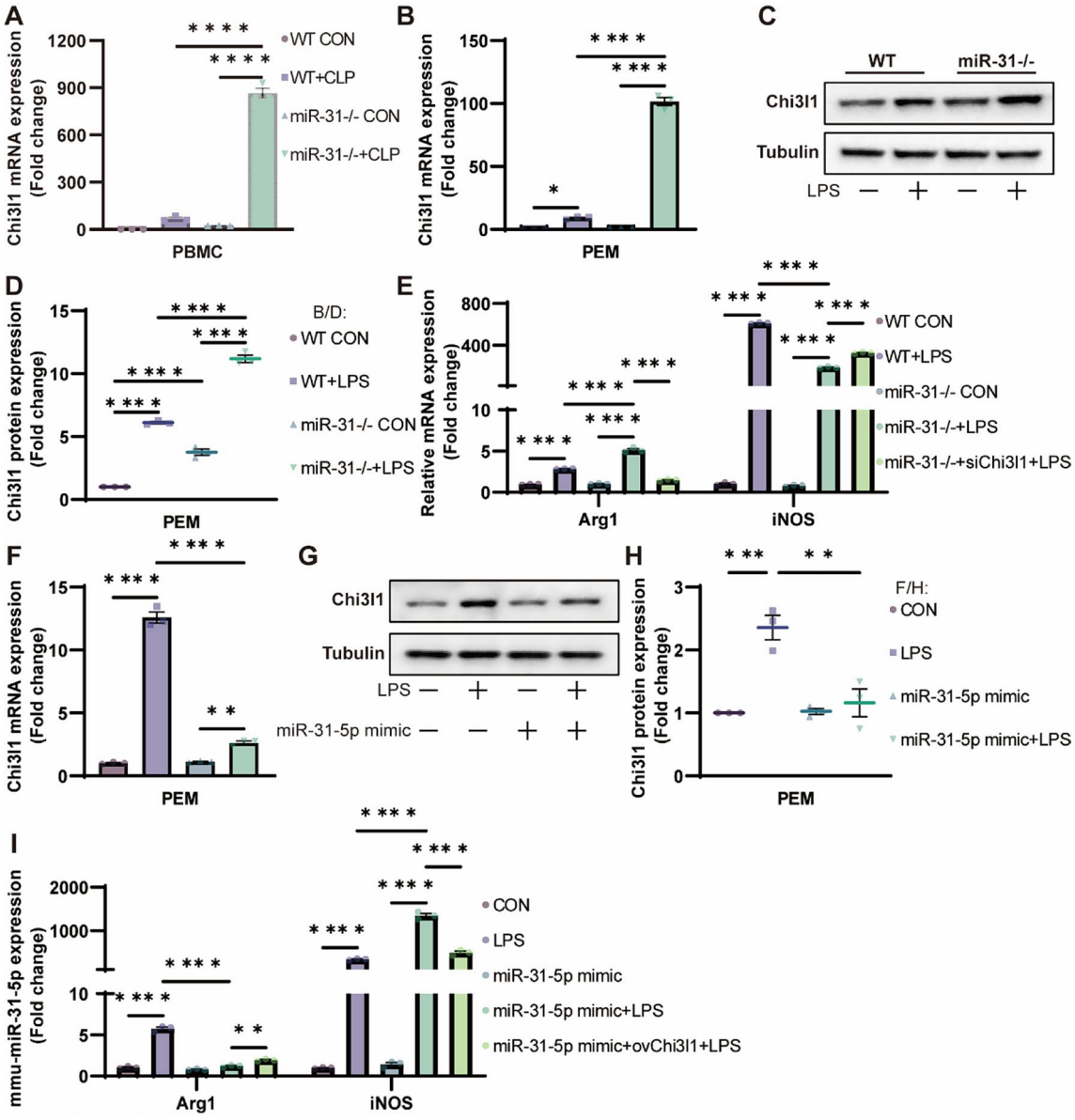

Fig. 5 miR-31 regulates macrophage polarization to M2 through Chi3l1. **A**. The mRNA expression of Chi3l1 in PBMCs of miR-31$^{-/-}$ mice with CLP was assayed. **B**, **C** and **D**. The mRNA and protein expression of Chi3l1 in PEMs isolated from miR-31$^{-/-}$ mice stimulated with 100 ng/ml LPS for 48 h were detected. **E**. The Chi3l1 overexpression plasmid to increase the expression of Chi3l1 in PEMs isolated from WT and miR-31$^{-/-}$ mice, then the mRNA expression of Arg1 and iNOS in PEMs with or without 100 ng/ml LPS for 48 h were detected. **F**, **G** and **H**. The mRNA and protein expression of Chi3l1 in miR-31-5p-overexpressing PEMs stimulated with 100 ng/ml LPS for 48 h were assayed. **I**. miR-31-5p mimic was used to increase the expression of miR-31-5p, then the mRNA expression of Arg1 and iNOS in Chi3l1-overexpresssing PEMs stimulated with or without 100 ng/ml LPS for 48 h were assayed. The data are presented as the mean ± SEM. $n = 3$, *$P < 0.05$, **$P < 0.01$, ***$P < 0.001$, ****$P < 0.0001$

a pivotal role in facilitating miRNA binding and proper alignment for interaction with target gene messenger RNA [16]. We revealed that the inhibition of CHI3L1 by hsa-miR-31-5p was not observed following argonaute-2 (Ago2) depletion (Fig. 6C), indicating a direct inhibitory effect of miR-31-5p on CHI3L1 through a conventional mechanism. RNA immunoprecipitation (RIP) experiments were conducted to investigate the enrichment of targets bound to miRNAs by Ago2 in lysates of PEMs using an antibody specific to Ago2. This experiment revealed a significant enrichment of mmu-miR-31-5p and Chi3l1 expression levels in Ago2-conjugated beads compared to the IgG control group (Fig. 6D–G).

Collectively, these findings suggest that miR-31-5p targets CHI3L1 by binding to its 3'-UTR region.

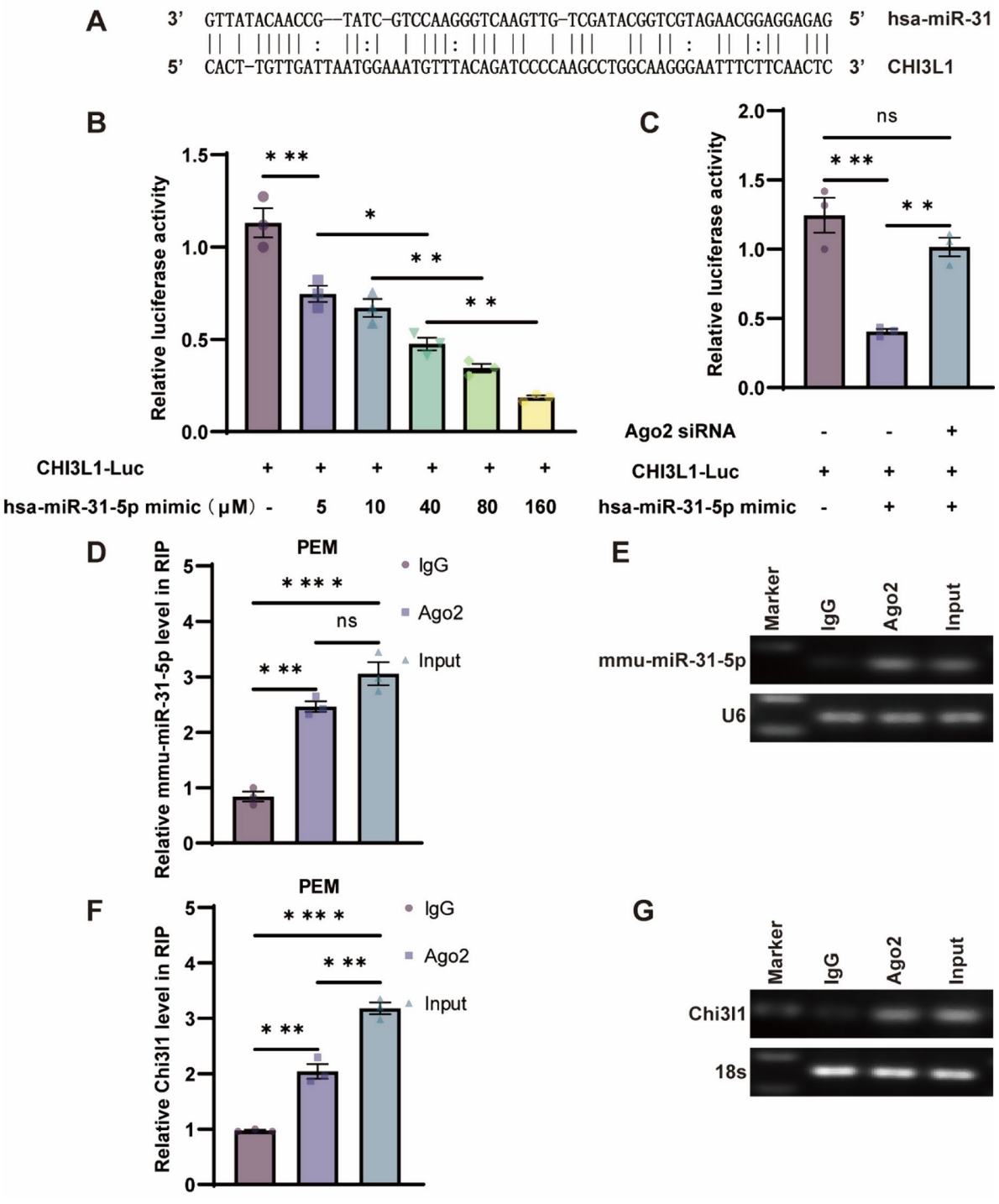

Fig. 6 miR-31-5p directly inhibits CHI3L1. **A**. Complementary sequences between hsa-miR-31-5p and the 3′ UTR of CHI3L1. **B**. CHI3L1 promoter luciferase reporter (CHI3L1-Luc) was co-transfected with miR-31-5p mimic in 293T cells for 24 h, and then relative luciferase activity was analyzed. **C**. The siRNA was used to inhibit the expression of Ago2, CHI3L1 promoter luciferase reporter (CHI3L1-Luc) was co-transfected with miR-31-5p mimic in Ago2-underexpressing 293T cells for 24 h, and then relative luciferase activity was analyzed. **D**, **E**, **F** and **G**. The association between Chi3l1, mmu-miR-31-5p and Ago2 was ascertained by analyzing PEMs lysates using RNA immunoprecipitation with an Ago2 antibody. qPCR was used to detect the change of Chi3l1 (**D**, **E**) and mmu-miR-31-5p (**F**, **G**) levels. The data are presented as the mean ± SEM. $n = 3$, $^{*}P < 0.05$, $^{**}P < 0.01$, $^{***}P < 0.001$, $^{****}P < 0.0001$

miPEP31 blocks mmu-miR-31-5p and protects against sepsis in mice

The miPEP31 encoded by pri-miRNA-31 acts as a transcriptional repressor, inhibiting miR-31-5p expression [17, 18]. To elucidate the regulatory influence of miPEP31 on mmu-miR-31-5p expression in macrophages, varying doses of synthetic miPEP31 were administered to PEMs, resulting in a dose-dependent decrease in miR-31-5p expression (Fig. 7A). Exploiting the targeting potential of miRNA offers promising avenues for sepsis diagnosis and treatment. Compared to exogenous drugs, miPEP31 demonstrates enhanced targeting capabilities with relatively lower antigenic characteristics.

To investigate the therapeutic potential of miPEP31 in sepsis, murine sepsis was induced via CLP followed by intravenous administration of miPEP31 at a dose of 50 μg immediately post-CLP. These findings indicate that miPEP31 administration in a murine sepsis model led to improved outcomes, as evidenced by enhanced prognosis (Fig. 7B and C) and reduced lung tissue injury in septic mice (Fig. 7D and E).

In vitro, pre-treatment of PEMs with miPEP31 followed by stimulation with 100 ng/ml LPS for 48 h resulted in a statistically significant increase in the mRNA and protein expression levels of Chi3l1 compared to the control group (Fig. 7F, G and H). Additionally, the expression levels of M1 markers in PEMs pre-treated with miPEP31 and stimulated with 100 ng/ml LPS for 48 h exhibited a reduction, whereas M2 markers showed an increase in comparison to the control group (Fig. 7I, J and K). Moreover, the concentrations of pro-inflammatory cytokines (IL-1β, IL-6, and TNF-α) in PEMs pre-treated with miPEP31 were reduced after being exposed to 100 ng/ml LPS for 48 h, in contrast to the control group. Conversely, the levels of the anti-inflammatory cytokine IL-10 were increased in the PEMs pre-treated with miPEP31 (Fig. 7L).

These results suggest that macrophages treated with miPEP31 exhibit a propensity to differentiate towards an M2 phenotype, potentially attenuating the inflammatory response.

Discussion

Sepsis is a multifaceted immune disorder initiated by pathogenic microorganisms, entailing intricate interactions of anti-inflammatory and pro-inflammatory responses mediated by diverse pathways and factors. Hence, effective management necessitates a comprehensive approach, recognizing that the efficacy of immunomodulatory drugs may vary depending on disease progression. Deciphering distinct immune response phases, identifying key markers, and targeting specific phases for precise immune modulation are important for successful sepsis immunotherapy. In this study, miRNAseq analysis revealed that septic patients showed significant downregulation of hsa-miR-31-5p compared to healthy controls, with a strong positive correlation between SOFA score/IL-6 and hsa-miR-31-5p levels in blood. We elucidated that miR-31-5p acts not only as a biomarker but also as a pivotal driver of sepsis, underscoring the potential of targeting specific miRNAs for sepsis treatment.

miRNAs exert diverse roles in sepsis pathophysiology, impacting immune responses, inflammation, tissue damage, and organ dysfunction. Understanding miRNA-mediated mechanisms in sepsis pathogenesis holds promise for novel diagnostic and therapeutic strategies. We revealed a significant reduction in miR-31-5p expression in septic patients compared to healthy individuals, with elevated levels correlating with sepsis mortality. The detectability of miR-31-5p suggests its utility as a diagnostic marker across different immune stages, warranting exploration of therapeutic agents targeting this molecule.

Recent research highlights miR-31's involvement in regulating Treg cell differentiation [17, 19], inflammatory signaling reduction [20], and colon epithelium regeneration [16]. Deletion of miR-31 in $CD4^+$ T cells enhances regulatory Treg cell induction and mitigates autoimmune encephalomyelitis severity [21]. Our study demonstrates significant changes in miR-31-5p expression in sepsis, impacting septic mouse survival, implicating its role in immune response regulation.

Furthermore, we reveals miR-31-5p's modulation of macrophage differentiation via Chi3l1, a pivotal immune mediator contributing to tissue remodeling and the pathogenesis of various inflammatory and autoimmune diseases [11]. Chi3l1's promotion of M2 macrophage differentiation underscores its importance, though its precise regulatory mechanism remains unclear. Our study unveils miR-31-5p's inhibition of Chi3l1 mRNA expression in sepsis, unveiling a previously unidentified regulatory pathway.

The miPEP31 encoded by pri-miRNA-31 acts as a transcriptional repressor, inhibiting miR-31-5p expression [17, 18]. Moreover, our findings indicate that miPEP31 protects against sepsis by inhibiting miR-31-5p expression. miPEP31 enhances septic mouse survival, attenuates macrophage inflammation, and promotes M2 macrophage polarization through Chi3l1 upregulation. Peptide drugs like miPEP31 offer advantages such as ease of synthesis, rapid optimization, reduced immunogenicity, and efficient clearance, suggesting their potential for sepsis treatment. miPEP31 represents a promising target for drug development, warranting further investigation into its specific mechanisms and potential clinical applications.

Although Chi3l1 alterations were observed in miR-$31^{-/-}$ mice, additional mechanisms may remain

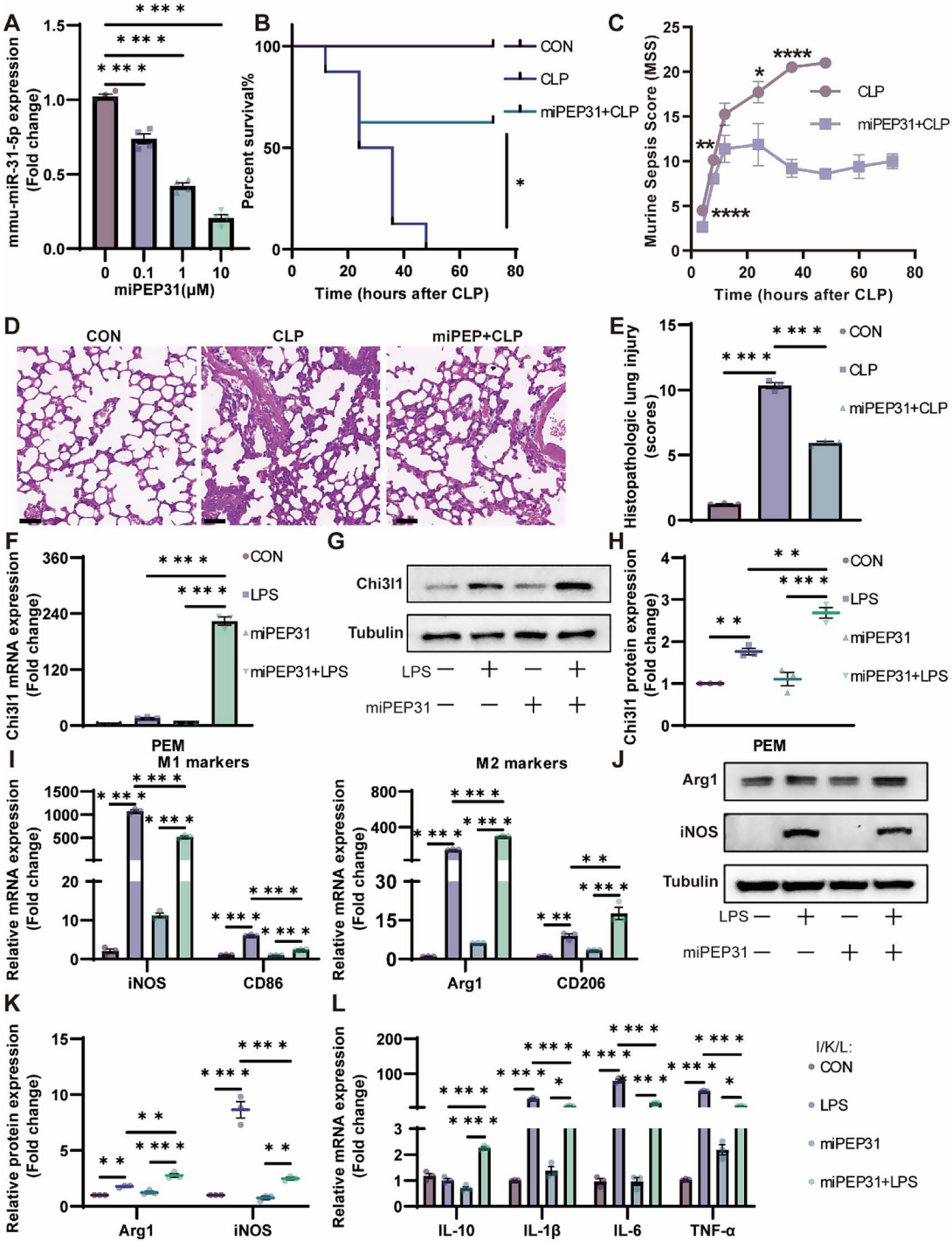

Fig. 7 miPEP31 blocks mmu-miR-31-5p and protects against sepsis in mice. **A**. mmu-miR-31-5p expression in PEMs treated by different dose of synthetic miPEP31 ($n=4$). **B**. The treatment with miPEP31 in mice increased the survival rate of mice with CLP (21-gauge needle)-induced sepsis (the data are presented as the mean ± SEM, $n=8$, mice per group; $^{*}P<0.05$, Kaplan–Meier survival analysis). **C**. Effects of miPEP31 on murine sepsis score (MSS) in mice with sepsis. Sepsis was induced by CLP (21-gauge needle) (the data are presented as the mean ± SEM, $n=8$, mice per group; $^{*}P<0.05$, $^{**}P<0.01$, $^{****}P<0.0001$). **D** and **E**. Lung tissues of mice with CLP-induced sepsis with or without treatment with miPEP31 were stained with hematoxylin and eosin (12 h; scale bars, 50 μm), and the histopathologic lung injury score. **F**, **G** and **H**. The mRNA and protein expression of Chi3l1 in PEMs pretreatment with miPEP31. **I**. The mRNA expression of Arg1, CD206, iNOS and CD86 in PEMs pretreatment with miPEP31. **J** and **K**. The protein expression of Arg1 and iNOS in PEMs pretreatment with miPEP31. **L**. The mRNA expression of IL-10, IL-1β, IL-6 and TNF-α in PEMs pretreatment with miPEP31. The data are presented as the mean ± SEM. $n=3$, $^{*}P<0.05$, $^{**}P<0.01$, $^{***}P<0.001$, $^{****}P<0.0001$

unexplored due to miR-31-5p's ability to target multiple genes. The mechanism by which Chi3l1 promotes M2 macrophage differentiation warrants further investigation, considering its involvement in receptor-dependent pathways and signaling cascades.

In summary, the results of this study suggest that inhibiting miR-31-5p holds promise as a beneficial strategy in sepsis by promoting M2 macrophage polarization, with Chi3l1 identified as a target gene of miR-31-5p. Further investigation is required to fully understand the precise mechanisms underlying this targeted correlation. Nonetheless, miR-31-5p emerges as a potential novel therapeutic target for sepsis, and miPEP31 may offer improvements in the management of individuals affected by this condition.

Limitation

The small sample size is a major limitation of this study section. We collected sepsis cases from viral pneumonia at our center between January and March 2023. After this, a sharp decline in such cases limited our ability to gather comparable data, resulting in a smaller clinical sample size. Future research will involve a comprehensive longitudinal collection of clinical cases to gather enough comparable or diverse sepsis samples to further validate the experimental system's efficacy.

Materials and methods

Patient samples

PBMCs were obtained from 10 sepsis patients and 5 healthy controls at Shanghai General Hospital from November 2022 to February 2023. Sepsis was diagnosed based on the criteria outlined in the Third International Consensus Definitions for Sepsis and Septic Shock (Sepsis-3). The study received approval from the Ethics Committee of Shanghai General Hospital under ethical approval number 2022SQ098. Patient characteristics can be found in Table 1.

Table 1 Clinical characteristics of non-septic patients and sepsis patients

	Control group ($n=5$)	Sepsis group (survivors, $n=5$)	Sepsis group (non-survivors, $n=5$)
Age, mean (SEM)	59.6(5.9)	72(3.3)	75(4.4)
Gender n%			
Male	3(60%)	4(80%)	3(60%)
Female	2(40%)	1(20%)	2(40%)
APACHE II, mean (SEM)	N/A	19.4(2.4)	32.2(4.3)
SOFA, mean (SEM)	N/A	6.8(1.4)	13.8(2.3)
GCS, mean (SEM)	N/A	11.2(1.3)	4.8(1.1)
Procalcitonin, mean (SEM)	N/A	3.2(1.8)	3.4(2.0)
CRP, mean (SEM)	N/A	128.6(44.7)	141.9(20.7)
WBC, mean (SEM)	N/A	11.7(2.1)	7.9(3.1)
IL-6, mean (SEM)	N/A	47.6(23.0)	1089.7(735.3)
ICU stay, days, median (range)	N/A	21(15–55)	24(21–28)

Animal models of sepsis

C57BL/6 wild-type mice were procured from Shanghai SLAC Laboratory Animal Co., while miR-31$^{-/-}$ mice were generously provided by Professor Honglin Wang of the Clinical Transformation Research Institute at Shanghai General Hospital. The mice were housed in groups of five per cage in a temperature-regulated facility, adhering to a 12-hour light-dark cycle. Strict measures were taken to maintain the mice and conduct experimental procedures under pathogen-free conditions. All protocols were conducted in compliance with the Guidelines for the Care and Use of Laboratory Animals established by the National Academy of Sciences, China, and were approved by the Experimental Animal Management Ethics Committee of Shanghai Jiao Tong University School of Medicine (ethical approval number: 2022AWS0160).

CLP model

Male wild-type and miR-31$^{-/-}$ mice (6–8 weeks old, weighing 20–25 g) were used to establish a model of polymicrobial sepsis through CLP following a previously described surgical protocol. Anesthesia was administered using sevoflurane (2–4% inhalation). The cecum was exposed through a small midline abdominal incision. The caecum was ligatured with 4−0 silk at either 75% (High-grade CLP, usually all mice die within 4 d after CLP induction) or 50% (Mid-grade CLP, 40% survival) and punctured with a 21-gauge needle [22]. The abdominal wall and skin were closed with sutures, the mice received a subcutaneous injection of 1 ml saline solution, and water and lab chow were reintroduced after the operation. After 12 h of CLP, the mice were euthanized with an overdose of pentobarbital (100 mg/kg). The tissue samples were preserved at a temperature of -80 °C in preparation for further analysis. Survival of the mice was monitored daily from Day 1 to Day 7 after the surgery. A humane endpoint was used for the CLP-treated mice.

Murine sepsis score

The murine sepsis score (MSS) was utilized in a murine sepsis model to forecast the onset of severe sepsis and mortality, as well as to evaluate the severity of sepsis [23]. The MSS encompasses the assessment of seven distinct criteria: appearance, level of consciousness, activity, response to a stimulus, aspect of the eyes, respiratory frequency, and respiratory quality. Each criterion was assigned a score ranging from 0 to 4, and the cumulative score was calculated. Mice were humanely euthanized if the MSS exceeded 21 at any given time point, or if there was a notable increase of more than 3 points in the scores

attributed to respiratory rate or quality. The deceased rodents were assigned a value of 21 points.

Cell culture

The HEK-293T cell line was procured from the Cell Bank of the Chinese Academy of Sciences and cultured in DMEM supplemented with 10% fetal bovine serum (FBS) and 1× penicillin-streptomycin. The cells were maintained in a CO2 incubator at 37 °C as part of routine culture procedures.

Following the established procedures for Ficoll density gradient centrifugation, PBMCs were isolated from human blood samples using lymphocyte separation medium. PEMs were obtained from wild-type or miR-31$^{-/-}$ mice, washed with phosphate-buffered saline (PBS), and cultured in Dulbecco's Modified Eagle Medium (DMEM) supplemented with 10% fetal bovine serum (Gibco) and 1× penicillin-streptomycin. The PEMs were then seeded into 6-well culture plates and treated with LPS (Sigma, #L2630) at a concentration of 100 ng/ml for 48 h following a 1-day culture period.

In vitro phagocytosis assay

The phagocytosis of macrophages was determined using a Vybrant™ Phagocytosis Assay Kit (Life Technologies™) according to the manufacturer's instruction. Briefly, PEMs were cultured in 96-well black culture plate at 1×10^6 cells/well. The cells were incubated for 48 h with LPS 100 ng/ml. The negative control (only DMEM) was prepared. Culture medium was removed and fluorescein-labeled Escherichia coli Bio Particles were added. After 120 min, supernatant was removed and 100 µl of trypan blue was immediately added to each well for 1 min to quench extracellular fluorescence. Excess trypan blue dye was removed by aspiration. The plate was read on FLUO star OPTIMA microplate reader at 480 nm excitation and 520 nm emission. Results are expressed as the percentage of phagocytosis relative to the untreated cells.

Western blot

The cells and tissues underwent washing with 1× PBS followed by lysis in RIPA lysis buffer supplemented with protease inhibitors. Subsequently, the cell lysates were subjected to separation by SDS-PAGE, transfer onto PVDF membranes, and immunoblotting using specific antibodies. The antibodies utilized included Chi3l1 (1:1000; #12036-1-AP, Proteintech), α-tubulin (1:40000; #66031-1-Ig, Proteintech), Arg1 (1:5000; #16001-1-AP, Proteintech), and iNOS (1:500; # sc-7271, Santa Cruz).

Quantitative real-time PCR

RNA was extracted from samples using TRIzol reagent (#9109, TAKARA), followed by reverse transcription of 1 µg of RNA to generate cDNA (#R323-01-AC, Vazyme). The resulting cDNA was then subjected to qRT-PCR using SYBR Green Master Mix (#Q711-02-AA, Vazyme), with primer sequences detailed in Table 2.

Cell transfection

The Chi3l1 gene and its overexpression plasmid were inserted into the pCDNA3.1 vector containing a Flag tag. Small interfering RNA sequences targeting Chi3l1, specifically 5'-GGAGUUUAAUCUCUUGCAA-3' and 5'-UUGCAAGAGAUUAAACUCC-3', were transfected into PEMs using Lipofectamine 8000 reagent (#C0533, Beyotime Biotechnology) to downregulate Chi3l1 expression and induce Chi3l1 overexpression. Following transfection, all cells were exposed to LPS stimulation for 48 h.

Luciferase reporters

293T cells were seeded at a density of 5×10^4 cells per well in a 24-well plate and co-transfected with hsa-miR-31-5p mimics and plasmids containing fragments of the human CHI3L1 promoter (pCHI3L1(human)-Fluc) using Lipofectamine 8000 reagent (#C0533, Beyotime Biotechnology). Following transfection, cells were incubated for 24 h and luciferase activity was quantified using the

Table 2 Sequences of the primers used for this study

Gene	Forward sequence 5'–3'	Reverse sequence 5'–3'
U6	CTCGCTTCGGCAGCACA	AACGCTTCACGAATTTGCGT
hsa-miR-31-5p	GTCGTATCCAGTGCAGGGTCCGAGGTA	AGTGCAGGGTCCGAGGTATT
mmu-miR-31-5p	CTCGGATCCTGTGCATAACTGCCTTCA	CACAAGCTTGAAGTCAGGGCGAGACAGAC
18s	GTAACCCGTTGAACCCCATT	CCATCCAATCGGTAGTAGCG
TNF-α	CCCTCACACTCAGATCATCTTCT	GCTACGACGTGGGCTACAG
IL-6	TAGTCCTTCCTACCCCAATTTCC	TTGGTCCTTAGCCACTCCTTC
IL-10	GCCTTATCGGAAATGATCCA	AGGGGAGAAATCGATGACAG
IL-1β	TGGACCTTCCAGGATGAGGACA	GTTCATCTCGGAGCCTGTAGTG
Chi3l1	AGACGCCATCCAACCTTTCC	GTTCGACTCGTCATTCCACTC
Arg-1	AAGAATGGAAGAGTCAGTGTGG	GGGAGTGTTGATGTCAGTGTG
iNOS	GAGACAGGGAAGTCTGAAGCAC	CCAGCAGTAGTTGCTCCTCTTC
CD206	GTTCACCTGGAGTGATGGTTCTC	AGGACATGCCAGGGTCACCTTT
CD86	ACGTATTGGAAGGAGATTACAGCT	TCTGTCAGCGTTACTATCCCGC

Dual Luciferase Reporter Assay System Kit (#DL101-21, Vazyme).

RNA immunoprecipitation (RIP)

The RIP assay was performed using a commercial RIP kit (BersinBio, Guangzhou, China). The PEM cell lysates were incubated with 5 μg of argonaute-2 (Ago2) antibody (#67934-1-Ig, Proteintech) or control anti-immunoglobulin G (IgG) antibody-coated beads at 4 °C overnight with rotation. Subsequently, total RNA was collected to analyze the expression levels of mRNA and miRNA via RT-qPCR.

Peptide assays

The peptides were synthesized by ChinaPeptides™ and were dissolved at 10 mM in sterile water. The molecular weight was confirmed by a mass spectrometer, and the purity was over 95%.

Peptide sequences

miPEP31: MRDWASVSSLGSGLWKERLWKSITTKRDGIAPVTRNW RGGKMLA; scrambled miPEP31 (scPEP): GWRTKDWSISPLKAVLGWIRTSG GDTRMNKLARLAKESWVRSMG; scPEP and miPEP31 have the same amino acid composition and quantity, with the only difference being that the sequence of amino acids in scPEP is randomly shuffled [17].

Tail vein injection

ScPEP (control peptide) or miPEP31 (50 μg) was intravenously injected into C57BL/6 mice through the tail vein with a 100-μL phosphate-buffered saline volume.

Bioinformatics and statistical analyses

The results were presented as the mean±standard error of the mean (SEM). Statistical analysis was carried out using GraphPad Prism 9 software. Unpaired two-tailed Student's t-tests were utilized to compare two samples, while one-way analysis of variance (ANOVA) was employed for comparisons among multiple groups. Kaplan-Meier analysis was used to assess differences in survival rates between groups. Statistical significance was determined at a *P*-value of less than 0.05.

Abbreviations

Ago2	Argonaute-2
Arg1	Arginase-1
Chi3l1	Chitinase-3-like 1
CLP	Caecal ligation and puncture
DMEM	Dulbecco's Modified Eagle Medium
FBS	Fetal bovine serum
ICU	Intensive care unit
IFN-γ	Interferon-gamma
IL-10	Interleukin-10
IL-13	Interleukin-13
IL-1β	Interleukin-1beta
IL-4	Interleukin-4
IL-6	Interleukin-6
LPS	Lipopolysaccharide
miRNAs	MicroRNAs
MSS	Murine sepsis score
PAMP	Pathogen-associated molecular pattern
PBMCs	Peripheral blood mononuclear cells
PBS	Phosphate-buffered saline
PEMs	Peritoneal elucidated macrophages
RIP	RNA immunoprecipitation
RISC	RNA-induced silencing complex
SOFA	Sequential organ failure assessment
TNF-α	Tumour necrosis factor-alpha
WT	Wild-type

Supplementary Information

The online version contains supplementary material available at https://doi.org/10.1186/s13062-024-00568-w.

Supplementary Material 1

Acknowledgements

We thank Honglin Wang and Hong Zhou (Precision Research Center for Refractory Diseases, Institute for Clinical Research, Shanghai General Hospital, Shanghai Jiao Tong University School of Medicine) for providing the miR-31$^{-/-}$ mice and miPEP31. We also express our gratitude to Yuqi Liu and Lijuan Wang for their valuable assistance with experimental technical guidance.

Author contributions

Y.Z., J.L., and F.C. conceived and planned the experiments. Y.Z., Y.Y., X.Y., and L.W. carried out the simulations and sample preparation, and analyzed the data. Y.Z. performed clinical sample assays. Y.Z., Y.Y., and L.Y. edited the manuscript and contributed to the interpretation of the results. Y.Z., J.L., D.T., and F.C wrote the paper.

Funding

This research received funding from the National Natural Science Foundation of China (81971813 and 82272193).

Data availability

No datasets were generated or analysed during the current study.

Declarations

Ethics approval and consent to participate

All procedures performed in studies involving human participants were approved by the Ethics Committee of Shanghai General Hospital under ethical approval number 2022SQ098. All animal experiments were conducted under the rules approved by the Experimental Animal Management Ethics Committee of Shanghai Jiao Tong University School of Medicine (ethical approval number: 2022AWS0160).

Consent for publication

All authors listed have provided their consent for submission, and all data utilized in this study have been obtained with the consent of the individuals responsible for generating the data.

Competing interests

The authors declare no competing interests.

Author details

[1]Department of Anesthesiology, Shanghai General Hospital, Shanghai Jiao Tong University School of Medicine, Shanghai 200080, China
[2]Department of Surgery, UT Southwestern Medical Center, Dallas, TX 75390, USA

Received: 18 July 2024 / Accepted: 13 November 2024
Published online: 18 November 2024

References

1. Singer M, Deutschman CS, Seymour CW, Shankar-Hari M, Annane D, Bauer M, Bellomo R, Bernard GR, Chiche JD, Coopersmith CM, et al. The Third International Consensus definitions for Sepsis and septic shock (Sepsis-3). JAMA. 2016;315(8):801–10.
2. Baghdadi JD, Brook RH, Uslan DZ, Needleman J, Bell DS, Cunningham WE, Wong MD. Association of a care bundle for early Sepsis Management with Mortality among patients with Hospital-Onset or Community-Onset Sepsis. JAMA Intern Med. 2020;180(5):707–16.
3. Rudd KE, Johnson SC, Agesa KM, Shackelford KA, Tsoi D, Kievlan DR, Colombara DV, Ikuta KS, Kissoon N, Finfer S, et al. Global, regional, and national sepsis incidence and mortality, 1990–2017: analysis for the global burden of Disease Study. Lancet (London England). 2020;395(10219):200–11.
4. Chen H, Zhang X, Su H, Zeng J, Chan H, Li Q, Liu X, Zhang L, Wu WKK, Chan MTV. Immune dysregulation and RNA N6-methyladenosine modification in sepsis. Wiley Interdiscip Rev RNA. 2023;14(3):e1764.
5. Chen X, Liu Y, Gao Y, Shou S, Chai Y. The roles of macrophage polarization in the host immune response to sepsis. Int Immunopharmacol. 2021;96:107791.
6. Lu TX, Rothenberg ME. MicroRNA. J Allergy Clin Immunol. 2018;141(4):1202–7.
7. Formosa A, Turgeon P, Dos Santos CC. Role of miRNA dysregulation in sepsis. Mol Med. 2022;28(1):99.
8. Iro MA, Soundara Pandi SP. Clinical application of non-coding RNAs in sepsis. Curr Opin Infect Dis. 2020;33(6):530–9.
9. Kingsley SMK, Bhat BV. Role of microRNAs in sepsis. Inflamm Research: Official J Eur Histamine Res Soc [et al]. 2017;66(7):553–69.
10. Essandoh K, Li Y, Huo J, Fan GC. MiRNA-Mediated macrophage polarization and its potential role in the regulation of inflammatory response. Shock (Augusta Ga). 2016;46(2):122–31.
11. Zhao T, Su Z, Li Y, Zhang X, You Q. Chitinase-3 like-protein-1 function and its role in diseases. Signal Transduct Target Ther. 2020;5(1):201.
12. Yu JE, Yeo IJ, Han SB. Significance of chitinase-3-like protein 1 in the pathogenesis of inflammatory diseases and cancer. Exp Mol Med. 2024;56(1):1–18.
13. Zhao H, Huang M, Jiang L. Potential roles and future perspectives of chitinase 3-like 1 in macrophage polarization and the Development of diseases. Int J Mol Sci. 2023;24(22).
14. Kim MJ, Shim DH. Chitinase 3-like 1 protein plays a critical role in respiratory syncytial virus-induced airway inflammation. Allergy. 2019;74(4):685–97.
15. Rehli M, Niller HH, Ammon C, Langmann S, Schwarzfischer L, Andreesen R, Krause SW. Transcriptional regulation of CHI3L1, a marker gene for late stages of macrophage differentiation. J Biol Chem. 2003;278(45):44058–67.
16. Gregory RI, Chendrimada TP, Cooch N, Shiekhattar R. Human RISC couples microRNA biogenesis and posttranscriptional gene silencing. Cell. 2005;123(4):631–40.
17. Zhou H, Lou F, Bai J, Sun Y, Cai W, Sun L. A peptide encoded by pri-miRNA-31 represses autoimmunity by promoting T(reg) differentiation. EMBO Rep. 2022;23(5):e53475.
18. Liu Y, Wang L, Zhou C, Yuan Y, Fang B, Lu K, Xu F, Chen L, Huang L. MiR-31-5p regulates the neuroinflammatory response via TRAF6 in neuropathic pain. Biol Direct. 2024;19(1):10.
19. van der Heide V, Möhnle P, Rink J, Briegel J, Kreth S. Down-regulation of MicroRNA-31 in CD4 + T cells contributes to Immunosuppression in Human Sepsis by promoting TH2 skewing. Anesthesiology. 2016;124(4):908–22.
20. Zhan CY, Chen D, Luo JL, Shi YH, Zhang YP. Protective role of down-regulated microRNA-31 on intestinal barrier dysfunction through inhibition of NF-κB/HIF-1α pathway by binding to HMOX1 in rats with sepsis. Mol Med (Cambridge Mass). 2018;24(1):55.
21. Zhang L, Ke F, Liu Z, Bai J, Liu J, Yan S, Xu Z, Lou F, Wang H, Zhu H, et al. MicroRNA-31 negatively regulates peripherally derived regulatory T-cell generation by repressing retinoic acid-inducible protein 3. Nat Commun. 2015;6:7639.
22. Rittirsch D, Huber-Lang MS, Flierl MA, Ward PA. Immunodesign of experimental sepsis by cecal ligation and puncture. Nat Protoc. 2009;4(1):31–6.
23. Shrum B, Anantha RV, Xu SX, Donnelly M, Haeryfar SM, McCormick JK, Mele T. A robust scoring system to evaluate sepsis severity in an animal model. BMC Res Notes. 2014;7:233.

Publisher's note